Applied Catalysis A: General 489 (2015) 247–254

Contents lists available at ScienceDirect

Applied Catalysis A: General

journal homepage: www.elsevier.com/locate/apcata

Pd/K/Co-oxide catalyst for water gas shift

Eugene Kono, Sakurako Tamura, Keisuke Yamamuro, Shuhei Ogo, Yasushi Sekine*

Applied Chemistry, Waseda University, 3-4-1, Okubo, Shinjuku, Tokyo, Japan

ARTICLE INFO

Article history:
Received 11 July 2014
Received in revised form 8 October 2014
Accepted 9 October 2014
Available online 3 November 2014

Keywords:
Water gas shift
Cobalt catalyst
Potassium addition
In situ IR

ABSTRACT

Various Co_3O_4 catalysts were investigated for the water gas shift (WGS) reaction for hydrogen production. Although the catalyst supporting only palladium (Pd/Co_3O_4) showed low catalytic activity and higher selectivity to methanation, $Pd/K/Co_3O_4$ catalyst, with loading of potassium exceeding 0.78 wt%, showed high catalytic activity for the WGS reaction. Catalysts on which Pd and K exist closely showed high activity, as confirmed using various preparation methods. Results of XPS measurements for $Pd/K/Co_3O_4$ revealed that supported potassium donated electrons to Pd and Co. The state of CO adsorption species was affected by the potassium loading, resulting in high catalytic activity for the $Pd/K/Co_3O_4$ catalyst. These effects gave the $Pd/K/Co_3O_4$ catalyst high catalytic activity for the WGS reaction. That reaction over $Pd/K/Co_3O_4$ proceeds via surface cobalt carbonyl and then formate intermediates, as revealed by the TG and isotope exchange measurements using $H_2{}^{18}O$ and DRIFT.

1. Introduction

Hydrogen energy society has attracted attention in recent years. Fuel cells that can function at a low temperature like as a polymer electrolyte membrane fuel cell (PEMFC), requires high-purity hydrogen in the reformed gas because CO deactivates Pt electrodes. Therefore, the CO concentration in the reformed gas must be decreased [1–3]. Water–gas shift (WGS) (Eq. (1)) is an important reaction for obtaining hydrogen rich gas from the reformate. Additionally, this reaction is used for controlling the H_2/CO ratio of synthesis gas in C_1 chemistry.

$$CO + H_2O \leftrightarrow CO_2 + H_2 \quad \Delta H^0_{298.15} = -41.2\ \mathrm{kJ\,mol^{-1}} \tag{1}$$

This reaction is exothermic. For that reason, lower temperatures are favorable for high CO conversion because of the thermodynamic equilibrium limitation of WGS reaction. In a typical industrial process, the WGS reaction proceeds through two stages to achieve high CO conversion: a high-temperature shift (HTS) and a low-temperature shift (LTS). The first stage, using HTS catalyst like as Fe_2O_3–Cr_2O_3 catalyst, operates at 593–723 K [4]. Fe_2O_3–Cr_2O_3 catalyst reduces the CO concentration in the reformate to 1–5%. The Fe_2O_3–Cr_2O_3 catalyst is inexpensive, but CO conversion is low because of the thermodynamic equilibrium caused by the higher working temperature. Thermal sintering of the iron crystallites easily deactivates Fe_2O_3–Cr_2O_3 [1]. The LTS reaction, using $Cu/ZnO/Al_2O_3$ catalyst, operates at 363–523 K to reduce the CO concentration below 0.5%. $Cu/ZnO/Al_2O_3$ catalyst is deactivated easily by sintering of copper and poisoning by sulfur [1,5]. Therefore, a catalyst that can be operated through a one-step process at moderate temperatures and which has a suitable high activity is eagerly sought for use with the WGS reaction.

Catalysts operated at mid-range temperatures have been investigated by many researchers. Numerous reports describe catalysts using noble metal on metal oxide for the WGS reaction [6–10]. Several are Pt, Pd, and Rh on CeO_2 [8] and Au-supported metal oxide (Fe_2O_3, Co_3O_4, TiO_2, ZrO_2) [11]. Those reports describe that the reaction over these catalysts proceeded through a redox mechanism, in which the adsorbed CO on noble metal was oxidized to CO_2 by the lattice oxygen on the support. The oxygen vacancy of the support was oxidized by H_2O.

The promotion effect of alkali metal or alkaline-earth metal on noble metal catalysts for the WGS reaction at middle temperature has been investigated in many studies [12–16]. Zhai et al. reported that Na impregnation on Pt–SiO_2 showed higher WGS activity than non-promoted Pt-SiO_2. The addition of alkali metal strengthened the interaction between Pt and the support, and suitable active sites were created [16]. Panagiotopoulou and Kondarides reported that alkali metal interacts strongly with the TiO_2 surface and new active sites that consist of oxygen defect vacancy, noble metal, and support are created at the metal–support interface for the WGS reaction [14].

Our previous study revealed that $Pd/K/Fe_2O_3$ catalyst showed high activity for the WGS reaction at the moderate temperature of 573 K [17]. We demonstrated that the impregnation of Pd

* Corresponding author. Tel.: +81 3 5286 3114; fax: +81 3 5286 3114.
E-mail address: ysekine@waseda.jp (Y. Sekine).

http://dx.doi.org/10.1016/j.apcata.2014.10.016
0926-860X/

and K enhanced the redox properties of Fe_2O_3 and increased the WGS activity. The addition of Pd and K promoted the reduction of the metal oxide and the re-oxidation of the lattice oxygen by H_2O [18]. The Pd/K/Co_3O_4 catalyst showed higher activity than the Pd/K/Fe_2O_3 catalysts [19]. Additionally, the activities did not depend on the Pd loading weight. Catalysts that load potassium exceeding 0.78 wt% have high activity for the WGS reaction. Furthermore, the addition of potassium inhibited methane formation. Pd/K/Co_3O_4 shows a different trend from that of Pd/K/Fe_2O_3. We investigated the reasons why the Pd/K/Co_3O_4 catalyst has high activity for the WGS reaction by catalytic activity tests and characterization including TPR, XPS, and XAFS. The reaction mechanism was ascertained using Q-Mass and DRIFTS.

2. Experimental

2.1. Catalyst preparation method

The Pd/K/Co_3O_4 catalysts were prepared using an impregnation method. A commercial Co_3O_4 (Kanto Chemical Co. Inc.) was used as a catalyst support. Potassium-supported catalysts were prepared by impregnation with an aqueous solution of precursor salt, K_2CO_3 (Kanto Chemical Co. Inc.). The resulting slurry was dried on a hot plate under continuous stirring with subsequent calcination at 773 K for 1 h. Following that, Pd was impregnated on potassium-supported catalysts with an acetone solution of Pd $(OCOCH_3)_2$ (Kanto Chemical Co. Inc.). The resulting slurry was dried on a hot plate under continuous stirring with subsequent calcination at 773 K for 1 h. The loading amount of potassium was fixed to 0.78 wt%. The loading of Pd was 0.27, 0.53, 1.1, or 2.1 wt%. For the standard impregnation, potassium was impregnated first and then Pd was impregnated. For reverse impregnation, Pd was impregnated first.

To investigate the structure of K and Pd as active sites, other catalysts were prepared using a physical mixture of 2.2 wt%Pd/Co_3O_4 and 1.56 wt%K/Co_3O_4. Each was prepared using the impregnation method, and mixed together at a 1:1 ratio using a planetary ball mill in a dry condition, or in 2-propanol solvent.

2.2. Catalytic activity tests

Catalytic activity tests were performed in a fixed bed flow reactor at atmospheric pressure. A Pyrex glass tube with 8 mm outer diameter and 6 mm inner diameter was used as a reactor. The catalyst (250–500 μm particle size) with an amount of 40 or 80 mg, was charged in the reactor. Reaction conditions were the following: H_2O:CO:H_2:N_2:Ar = 30:6:42:13:9; total flow rate = 178 mL min^{-1}; W/F = 1.50 or 2.99 g-cat h mol^{-1}; reaction temperature at 573 K. The product gas was analyzed using a GC-FID/TCD (GC-8A; Shimadzu Corp.).

2.3. Characterization of catalysts

The oxidation–reduction property of catalysts during reaction was investigated using thermogravimetry (TG; TGA-50; Shimadzu Corp.). The catalyst weight loss was measured under heating to 573 K, which is the reaction temperature (20 K min^{-1}, in Ar purge). When the temperature reached 573 K, hydrogen, CO or a simulated reaction gas (H_2O:CO:H_2:Ar = 7.2:2.4:16.8:73.6; total flow rate = 100 mL min^{-1}) was supplied. The catalyst weight was 20 mg for each case.

Metal dispersions of Pd were measured using CO chemisorption (BEL-CAT-55; BEL Japan Inc.). The stoichiometric factor of CO/Pd was assumed as 1.0 for the calculation of metal dispersion. All catalysts were reduced in hydrogen at 473 K for 30 min and cooled to 323 K in He flow. Then, 10% CO/He was dosed 20 times in He flow.

X-ray photoelectron spectroscopy (XPS) measurements were conducted using a PHI-5000 VersaProbe II (ULVAC-Phi Inc.), with 25 W Al Kα emission as the X-ray source, to measure each electron state on the catalyst surface. After reaction, the catalysts were treated in the reaction condition for 185 min and cooled to room temperature in Ar purge. After reaction, the samples were carried by a transfer-vessel filled with N_2 to avoid air exposure. Binding energies were calibrated with a C 1s peak at 284.8 eV.

To observe the fine structures of Pd, K, and Co, the X-ray absorption fine structure (XAFS) measurement was conducted at the BL14B2 station at SPring-8 (Hyogo, Japan). Each edge was measured using a transmission method. The catalyst was pressed into a pellet (7 mmϕ). Pellets used for measuring Co K-edge were diluted with BN, treated in the reaction condition (H_2O:CO:H_2:N_2:Ar = 30:6:42:13:9) for 65 min and cooled to room temperature in Ar purge. Then, the pellet was packed into a gas-barrier bag in N_2 atmosphere. XAFS data were analyzed using software (REX2000; Rigaku Corp.). Fourier transformation of k^3-weighted EXAFS spectra was obtained in the k-range of 0.3–1.2 nm.

2.4. Transient response experiment

Transient response experiments were conducted using a quadrupole mass spectroscopy (Q-Mass; QGA; Hiden Analytical Ltd.). The gas compositions were the following: reaction gas, H_2O:CO:H_2:He:Ar = 16.7:3.3:23.3:48.9:7.8, total flow rate of 300 mL min^{-1}; purge gas, He:Ar = 276.6:23.3, total flow rate of 300 mL min^{-1}.

Isotope exchange reaction experiments were conducted to determine the contribution of lattice oxygen to the WGS reaction. After heating of the catalyst to 573 K (5 K min^{-1}) in He purge, the reaction gas was supplied at 573 K for 1 h. Then, 30% $H_2{}^{18}O$ (purity 98%; Taiyo Nippon Sanso Corp.) was supplied for 10 min to exchange the lattice oxygen in/on the catalyst. The reaction gas was supplied again to detect the product gas. To observe the lattice oxygen behavior during reaction, the reaction gas containing $H_2{}^{18}O$ ($H_2{}^{16}O$:$H_2{}^{18}O$:CO:H_2:He:Ar = 11.2:5.5:3.3:23.3:48.9:7.8, total flow rate of 300 mL min^{-1}) was supplied at 573 K for 1 h. The product gas was detected using a Q-Mass. Nine parent peaks were scanned using a mass spectrometer: m/e = 2 (H_2), 15 (CH_4), 18 (H_2O), 20 ($H_2{}^{18}O$), 28 ($C^{16}O$), 30 ($C^{18}O$), 44 ($C^{16}O_2$), 46 ($C^{16}O^{18}O$), and 48 ($C^{18}O_2$).

2.5. DRIFT measurements

Adsorption species and reaction intermediates were investigated using diffuse reflectance infrared Fourier transform spectroscopy (DRIFT; FT/IR-4200; Jasco Corp.). The experiment conditions were 600–4000 cm^{-1} measurement range, 1 cm^{-1} measurement interval, 4 cm^{-1} limit of resolution, and 64 times cumulated numbers. A peak that appeared from 3500–4000 cm^{-1} was attributed to H_2O. This peak was corrected with a background peak that was measured before CO intake. The total gas flow was 100 mL min^{-1}. All catalysts were pre-reduced. The catalysts were heated to 673 K for 1 h in Ar purge, and were reduced by 10% H_2 for 30 min at 473 K.

The spectrum for CO adsorption was measured to observe on the surface adsorbed species of the catalyst. After the catalyst was reduced, 3% CO gas was supplied at 298 K. Then the spectrum was measured. The spectrum was measured until no spectrum change was observed.

To identify the peaks in each spectrum, H–D exchange measurements were conducted. After the catalyst was reduced and cooled to 298 K, the spectrum was measured under 3% CO gas flow for

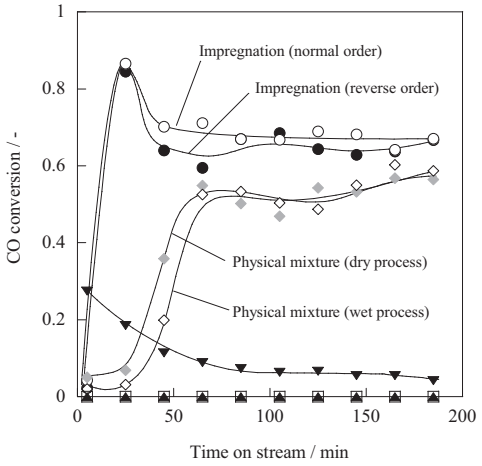

Fig. 1. Effects of catalyst preparation for various Pd–K–Co_3O_4 catalysts with loading amounts: Pd was 1.1 wt%; K was 0.78 wt%; ○, Pd/K/Co_3O_4; ●, K/Pd/Co_3O_4; ◊, physical mixture in 2-propanol of Pd/Co_3O_4 and K/Co_3O_4; ♦, physical mixture of Pd/Co_3O_4 and K/Co_3O_4; ▼, Pd/Co_3O_4; ▲, K/Co_3O_4;□, Co_3O_4.

30 min. Then, 4% H_2O or D_2O was supplied for 30 min at 573 K and cooled to 298 K to observe the spectrum.

3. Results and discussion

3.1. Relation to catalytic activity, preparation method and reducibility of cobalt oxide over Pd/K/Co_3O_4 catalysts

We demonstrated earlier that Pd/K/Co_3O_4 on which K loading had exceeded 0.78 wt% showed high catalytic activity for the WGS reaction and that the activity was independent of the Pd loading amount [19]. Based on that report, the influence of the preparation methods was investigated to ascertain the role of supported Pd and K. Fig. 1 presents results of activity tests over Pd/K/Co_3O_4 (Pd: 1.1 wt%, K: 0.78 wt%) prepared using various methods including different impregnation orders and physical mixture methods. We prepared Pd/K/Co_3O_4 using normal order impregnation, K/Pd/Co_3O_4 by reverse order impregnation, Pd/Co_3O_4 + K/Co_3O_4 by physical mixture (dry process) and physical mixture (wet process). The catalyst weight was 40 mg for each catalyst to avoid reaching the thermodynamic equilibrium. In Fig. 1, results show that the steady state activities on Pd/K/Co_3O_4 and K/Pd/Co_3O_4 are higher than those of other catalysts. The physical mixture catalysts (Pd/Co_3O_4 + K/Co_3O_4) showed moderate activity. These four catalysts (Pd/K/Co_3O_4, K/Pd/Co_3O_4, two catalysts by physical mixture of Pd/Co_3O_4 and K/Co_3O_4) showed >99% CO_2 selectivity, and methanation occurred only slightly. The initial activity of the catalyst by the physical mixture method was lower than that of the catalyst by the impregnation method because the supported Pd and K are more isolated over the catalyst prepared using the physical mixture method. Pd/Co_3O_4, K/Co_3O_4, and bare Co_3O_4 showed little or no catalytic activity for WGS. These data show that close contact between Pd, K, and Co is extremely important.

Although the Pd/K/Co_3O_4 showed high initial activity, the activity decreased over the course of time. Carbon deposition was negligibly small and did not influence the catalytic activity for the WGS reaction. The difference in activities at 5 and 185 min of the reaction suggests that the structure and/or state of Pd, K, and Co before and after the reaction changed in the reducing atmosphere (i.e. reaction gas includes CO). Therefore, the activity tests of pre-reduced Pd/K/Co_3O_4 by H_2 or CO before the reaction were performed to observe the relation to the reduction property of

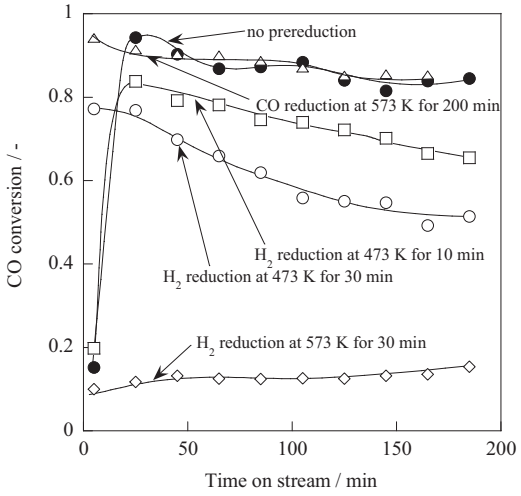

Fig. 2. Effect of pre-reduction for Pd/K/Co_3O_4: Pd, 1.1 wt%; K, 0.78 wt%.

support and the catalytic activity. Fig. 2 portrays the results of activity tests over pre-reduced Pd/K/Co_3O_4 (Pd: 1.1 wt%, K: 0.78 wt%) catalysts. Various pre-reduction conditions were investigated: 10% H_2 at 573 K for 30 min, 10% H_2 at 473 K for 30 min, 10% H_2 at 473 K for 10 min, and 10% CO at 573 K for 200 min. The catalyst weight was 80 mg for each catalyst. In Fig. 2, the catalyst which was reduced strongly by 10% H_2 for 30 min at 573 K showed the lowest activity. Results suggest that the activity of the catalyst which was reduced strongly was low because the catalyst support was reduced completely to form Co metal. CO conversion at 185 min of the catalyst was reduced slightly by about 10% H_2 at 473 K for 30 min, which was low compared to the catalyst without pre-reduction. On the other hand, the catalyst after reduction by CO gas showed higher activity at 5 min compared to the catalytic activity without reduction, and showed >99% CO_2 selectivity.

The reduction behavior of the catalyst was investigated using isothermal-TG (thermogravimetry) analyses at 573 K, the same as the reaction temperature, by supplying a simulated reaction gas to observe the reduction behavior of the support (Co_3O_4). Fig. 3 shows isothermal-TG profiles in the simulated reaction gas at 573 K over Co_3O_4, K/Co_3O_4, Pd/Co_3O_4 and Pd/K/Co_3O_4 (Pd: 1.1 wt%, K: 0.78 wt%). If the entire weight loss is attributable to the reduction of lattice oxygen in Co_3O_4, then the weight loss of −6.6 wt% is attributable to the reduction of Co_3O_4 to CoO, and −26.6 wt%

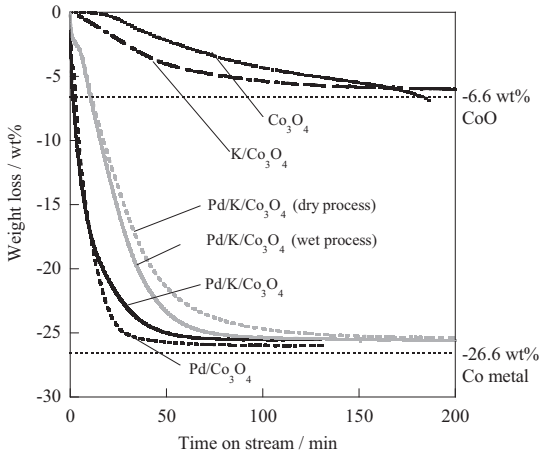

Fig. 3. TG profiles of various Pd/K/Co_3O_4 catalysts reduced by the simulated reaction gas: gray line, catalysts prepared using a physical mixture; black line, catalysts prepared using an impregnation method.

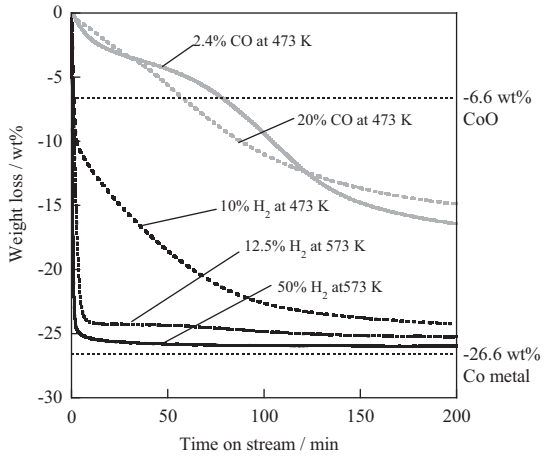

Fig. 4. TG profiles for $Pd/K/Co_3O_4$ reduced using various conditions: Pd, 1.1 wt%; K, 0.78 wt%; gray line, catalysts reduced by CO gas; black line, catalysts reduced by H_2 gas.

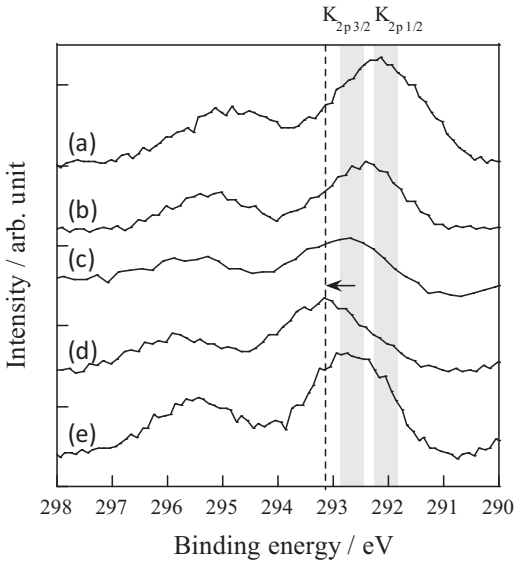

Fig. 5. XPS K 2p spectra of $Pd/K/Co_3O_4$ and K/Co_3O_4: (a) K/Co_3O_4 (as made), (b) $Pd/K/Co_3O_4$ (as made), (c) K/Co_3O_4 (after reaction), (d) $Pd/K/Co_3O_4$ (after reaction), and (e) $Pd/K/Co_3O_4$ (H_2 reduction).

is the reduction to Co metal. Although Co_3O_4 and K/Co_3O_4 on which Pd was not supported, were reduced to CoO, Pd/Co_3O_4 and $Pd/K/Co_3O_4$ were reduced to Co metal. Diehl and Khodakov have shown from TPR results that most noble metals can enhance the reduction of cobalt oxides [20]. Therefore, the reduction of cobalt oxide was promoted by the presence of Pd in this case as well. As a result of comparing the weight losses of $Pd/K/Co_3O_4$ catalysts prepared by the impregnation method and by the physical mixture method for 0–60 min, $Pd/K/Co_3O_4$ catalysts prepared using the impregnation method were more reducible than $Pd/K/Co_3O_4$ catalysts prepared using the physical mixture method. According to the result, the mutual proximity between Pd and K was important for the reducibility of cobalt oxide.

Next we conducted isothermal-TG analyses in an H_2 or CO atmosphere. Fig. 4 presents results of TG profiles over $Pd/K/Co_3O_4$ catalyst (Pd: 1.1 wt%, K: 0.78 wt%) during reduction by H_2 or CO under the constant temperature condition (i.e. 573 K, the same temperature as the reaction). In Fig. 4, the catalyst reduced by H_2 showed a decrease in weight to −26.6 wt%. Therefore, the support was reduced to Co metal by H_2 reduction. However, the catalyst reduced by CO showed decreased weight to −14 wt%. This reduction might result from the adsorption of CO on the catalyst surface.

To measure the amount of CO adsorption and metal dispersion of Pd, CO chemisorption was investigated. Table 1 presents results of CO chemisorption. Measurements were investigated after reduction by 30 mL min^{-1} H_2 at 473 K for 30 min of pre-reduction because the reaction condition was a reducing atmosphere. In Table 1, the CO adsorption amounts are shown to be independent of the Pd loading weight. Assuming the stoichiometric factor of CO/Pd as 1.0 for the calculation of metal dispersion and CO adsorbed only on Pd, the Pd dispersion of 0.27 wt%$Pd/K/Co_3O_4$ exceeded 100% dispersion, as shown in Table 1. This result indicates that CO adsorbed not only Pd but also Co support. However, CO could not be adsorbed onto Co_3O_4 and K/Co_3O_4. These results suggest that Pd over $Pd/K/Co_3O_4$ had some influence on the state of cobalt oxide. The amount of CO adsorption over $Pd/K/Co_3O_4$ catalysts increased compared to Pd/Co_3O_4. Therefore, it is estimated that CO adsorbed even onto Co because the electron state of Co was changed by the addition of potassium.

Table 1
Results of CO chemisorption of various catalysts.

	Pd loading (wt%)	Adsorption per unit (cm^3 g^{-1})	Pd dispersion (%)
Pd only	0.27	0.521	91.7
	0.53	0.518	46.4
	1.1	0.471	20.3
	2.1	0.563	12.7
Pd and K	0.27	1.241	218.3
	0.53	0.983	89.2
	1.1	1.468	63.4
	2.1	1.462	32.9
K/Co_3O_4	0.065	–	
Co_3O_4	0	–	

From these three experiments, i.e. catalytic activities after the reduction by CO, isothermal-TG profile in CO atmosphere, and CO-adsorption; we assume the reason why the catalyst pre-reduced by CO showed high WGS activity, because CO reduced the catalyst surface, adsorbed onto the catalytic surface, and the adsorbed CO produced active intermediates on the catalyst. This phenomenon was confirmed by results of DRIFT measurements presented in Section 3.3.

3.2. Characterization of catalysts

To clarify the effect of the electronic state of the catalyst surface on the activity and formation of adsorption intermediate, XPS measurements were conducted. Table 2 shows the binding energies of respective peaks for $Pd/K/Co_3O_4$, Pd/Co_3O_4, K/Co_3O_4, and Co_3O_4 (Pd: 1.1 wt%, K: 0.78 wt%). Fig. 5 shows the K 2p spectra of respective catalysts. The peak around 292.5–292.8 eV is attributable to K $2p_{3/2}$. The peak around 292.5 eV is attributable to K $2p_{1/2}$ [21,22]. In Fig. 5, the K $2p_{3/2}$ peaks on $Pd/K/Co_3O_4$ shifted to higher binding energy during the reaction, perhaps because of the decreasing electron density of the potassium site. Asano et al. reported that the K $2p_{3/2}$ peak shifted slightly toward the high binding energy side with increasing potassium loading, and reported that the electronic state of potassium changed on K/Co_3O_4 [23].

Fig. 6 shows Pd 3d spectra of respective catalysts. The peak at 335.5 eV is attributed to Pd metal. The peak at 336.8 eV is attributable to PdO [24]. The Pd $3d_{5/2}$ peak on $Pd/K/Co_3O_4$ catalysts shifted to lower binding energy compared to that of Pd/Co_3O_4 catalysts, irrespective of whether they were measured before and after the reaction. Previously, Pekiridis et al. reported that the Pd $3d_{5/2}$ peak shifted to lower binding energies along with increasing

Table 2
Binding energies of various catalysts.

Binding energy (eV)	$Pd/K/Co_3O_4$			Pd/Co_3O_4			K/Co_3O_4		Co_3O_4	
	As made	af. RUN	H_2 red	As made	af. RUN	H_2 red	As made	af. RUN	As made	af. RUN
Co 2p 3/2	779.4	781.1	780.7	780.2	781.5	779.8	779.8	780.5	780.4	780.3
	–	778.3	–	–	778.5	–	–	–	–	–
O 1s	–	531.9	531.1	–	531.9	531.0	–	–	–	–
	529.8	–	–	530.2	–	529.4	529.1	529.6	530.3	529.7
Pd 3d 3/2	342.2	340.8	340.3	342.9	341.7	340.6	–	–	–	–
Pd 3d 5/2	336.7	335.7	335.0	337.5	336.1	335.3	–	–	–	–
K 2p 1/2	295.0	295.9	295.5	–	–	–	294.8	295.3	–	–
K 2p 3/2	292.4	293.2	292.8	–	–	–	292.1	292.7	–	–
C 1s	284.8	284.8	284.8	284.7	284.8	284.8	284.8	284.8	284.8	284.8

K loading because the enhanced electron density of Pd sites for potassium promoted Pd/Al_2O_3 [25]. In our case, the higher electron density on Pd over $Pd/K/Co_3O_4$ catalyst was observed because of the electric donation from potassium to Pd. In addition, because the peak shift of $Pd/K/Co_3O_4$ catalyst appeared before reaction, the electric donation by potassium to Pd was known to have occurred during calcination.

The $3d_{5/2}$ peak over $Pd/K/Co_3O_4$ after reaction showed 0.7–0.8 eV higher binding energy than that of Pd metal. The XPS spectra of Pd–Co alloy were reported previously. The Pd $3d_{5/2}$ peak of Pd–Co alloy shifted to 0.4–0.6 eV higher binding energy compared to that of Pd metal [26–28]. Therefore, Pd and Co became alloyed during the reaction, whether potassium was present or not, because both $Pd/K/Co_3O_4$ and Pd/Co_3O_4 shifted to higher binding energy compared to Pd metal.

Fig. 7 presents Co 2p spectra of respective catalysts. The peak at 774–784 eV is attributable to Co $2p_{3/2}$. The Co $2p_{3/2}$ peak at 777.5–780 eV is attributable to Co^0, and the peak at 780.3–781.8 eV is attributable to CoO [29,30]. In Fig. 7, the Co $2p_{3/2}$ peak of K/Co_3O_4 and $Pd/K/Co_3O_4$ before the reaction shifted to lower binding energy than that of Co_3O_4 before the reaction. In addition, the Co $2p_{3/2}$ peak of $Pd/K/Co_3O_4$ after the reaction shifted to lower binding energy than that of Pd/Co_3O_4 after the reaction. According to these results, the addition of potassium increased the electron density of Co and cobalt accepted electrons from potassium whether Pd was present or not. For Co_3O_4 with loading of a small amount of potassium, the Co $2p_{3/2}$ peak shifted similarly to the lower binding energy side because of the changing electronic state of cobalt [23]. Consequently, these XPS results suggest that potassium donated electrons to Pd and Co, and suggest that Pd and Co became alloyed during the reaction.

To clarify the fine structure of Pd, XAFS measurements were investigated. Fig. 8 shows XANES spectra of Pd K-edge. Fig. 9 shows EXAFS spectra of Pd and Co K-edge. PdO, Pd foil, and Co foil were used as reference samples. $Pd/K/Co_3O_4$ and Pd/Co_3O_4 after reaction, with various Pd loading weights, were measured. In Fig. 8, the XANES spectra of $Pd/K/Co_3O_4$ catalyst or Pd/Co_3O_4 catalyst did not match the spectra of reference samples. This result shows that the fine structure of Pd over $Pd/K/Co_3O_4$ catalysts was neither PdO nor Pd metal. In Fig. 9, the EXAFS spectra of $Pd/K/Co_3O_4$ for Pd K-edge resembled the spectra of Co foil for Co K-edge. Formation of Pd–Co alloy was confirmed from this result, which is consistent with previous results obtained by several authors [31–33]. In their report, they have claimed that K-edge spectra of platinum group elements such as Pd, Ru, shifts towards a shorter atomic length due to the formation of a Co alloy. In our case, the loading amount of Pd is very little compared to the Co_3O_4 support; hence the Pd K-edge peak shifts nearly close to the peak of Co foil.

3.3. Reaction mechanism over $Pd/K/Co_3O_4$

As reaction mechanisms for the WGS reaction, two options are proposed: a redox mechanism and Langmuir–Hinshelwood mechanism. The reaction for the redox mechanism includes CO oxidation to CO_2 by the lattice oxygen and lattice oxygen regeneration by

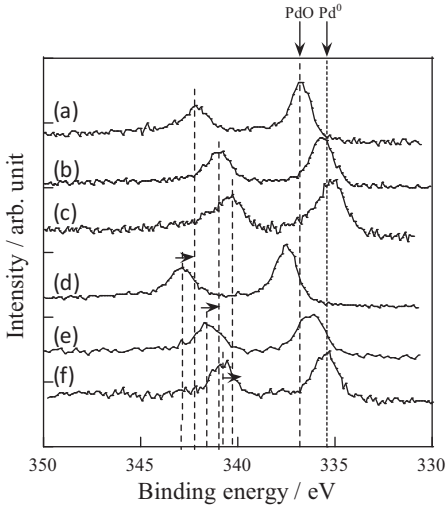

Fig. 6. XPS Pd 3d spectra of $Pd/K/Co_3O_4$ and Pd/Co_3O_4: (a) $Pd/K/Co_3O_4$ (as made), (b) $Pd/K/Co_3O_4$ (after reaction), (c) $Pd/K/Co_3O_4$ (H_2 reduction), (d) Pd/Co_3O_4 (as made), (e) Pd/Co_3O_4 (after reaction), and (f) Pd/Co_3O_4 (H_2 reduction).

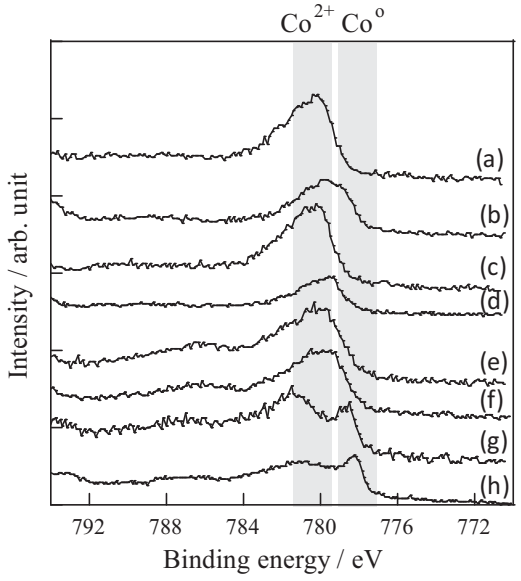

Fig. 7. XPS Co 2p spectra of $Pd/K/Co_3O_4$, Pd/Co_3O_4, Pd/Co_3O_4, and Co_3O_4: (a) Co_3O_4 (as made), (b) K/Co_3O_4 (as made), (c) Pd/Co_3O_4 (as made), (d) $Pd/K/Co_3O_4$ (as made), (e) Co_3O_4 (after reaction), (f) K/Co_3O_4 (after reaction), (g) Pd/Co_3O_4 (after reaction), and (h) $Pd/K/Co_3O_4$ (after reaction).

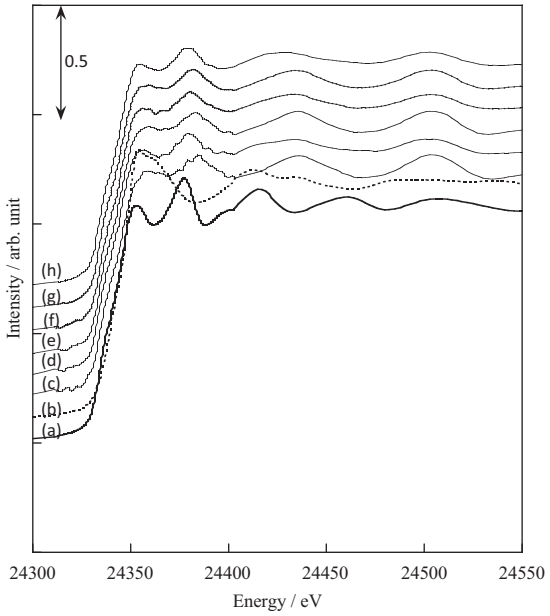

Fig. 8. XANES spectra for Pd K-edge of $Pd/K/Co_3O_4$ and Pd/Co_3O_4: (a) Pd foil, (b) PdO, (c) 0.53 wt%Pd/Co_3O_4, (d) 0.53 wt%$Pd/K/Co_3O_4$, (e) 1.1 wt%Pd/Co_3O_4, (f) 1.1 wt%$Pd/K/Co_3O_4$, (g) 2.1 wt%Pd/Co_3O_4, (h) 2.1 wt%$Pd/K/Co_3O_4$.

H_2O. The Langmuir–Hinshelwood mechanism proceeds via surface intermediates such as formate produced by adsorbed CO and H_2O on the catalyst surface [1]. We investigated which reaction mechanism proceeds over $Pd/K/Co_3O_4$ by steady state isotope kinetic analysis using $H_2{}^{18}O$ and Q-Mass, and DRIFT measurements.

To observe the lattice oxygen behavior during reaction over $Pd/K/Co_3O_4$ catalyst, isotope transient experiments over $Pd/K/Co_3O_4$ catalyst (Pd, 1.1 wt%; K, 0.78 wt%) were conducted using $H_2{}^{18}O$ and Q-Mass. Table 3 shows the results. After the reaction gas was supplied for an hour, $H_2{}^{18}O$ gas or the reaction gas containing $H_2{}^{18}O$ was supplied. Then, the reaction gas was flowed and the signal was observed by Q-Mass. Table 3 shows the total amounts of the first 10 signal products after switching the reaction gas after isotope exchange. If the reaction proceeds via the redox mechanism, then the lattice oxygen, which is replaced by isotope

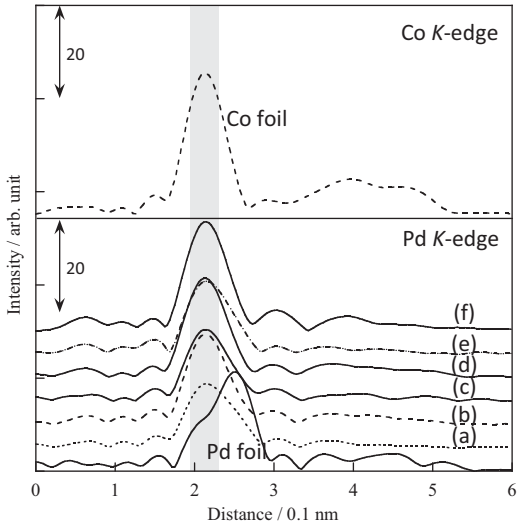

Fig. 9. EXAFS spectra for Pd K-edge of $Pd/K/Co_3O_4$ and Pd/Co_3O_4: (a) 2.1 wt%$Pd/K/Co_3O_4$, (b) 2.1 wt%Pd/Co_3O_4, (c) 1.1 wt%$Pd/K/Co_3O_4$, (d) 1.1 wt%Pd/Co_3O_4, (e) 0.53 wt%$Pd/K/Co_3O_4$, (f) 0.53 wt%Pd/Co_3O_4.

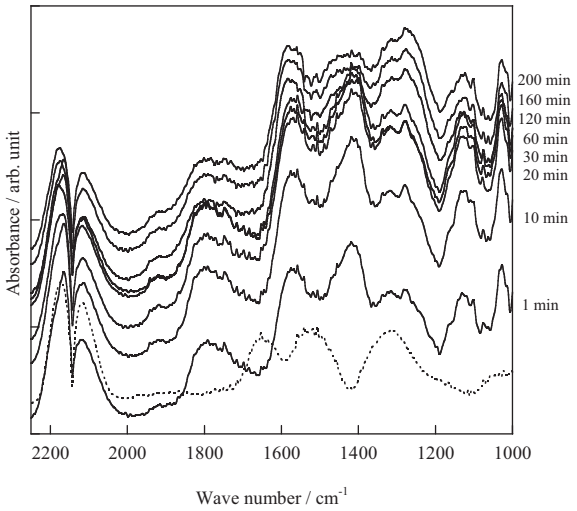

Fig. 10. DRIFT spectra of flowing CO gas at 573 K over $Pd/K/Co_3O_4$: dotted line, DRIFT spectra of CO adsorption at 298 K over $Pd/K/Co_3O_4$.

^{18}O, can react with the supplied gas, thereby producing $C^{16}O^{18}O$ and $C^{18}O_2$. In Table 3, the amounts of $C^{16}O^{18}O$ and $C^{18}O_2$ produced after isotope exchange were very small compared to the $C^{16}O_2$ produced after isotope exchange. Therefore, the lattice oxygen did not play an important role during the WGS reaction over $Pd/K/Co_3O_4$ catalyst. The reaction over $Pd/K/Co_3O_4$ proceeds not via the redox mechanism but via the Langmuir–Hinshelwood mechanism.

DRIFT measurements were investigated to ascertain the adsorbed species in detail. First, DRIFT spectra were observed by supplying 10%CO gas at 573 K after measuring the background at 298 K to reveal the reason why $Pd/K/Co_3O_4$ catalyst that had been pre-reduced by CO showed high catalytic activity even at the initial stage of WGS. Fig. 10 presents spectra during CO supplying over $Pd/K/Co_3O_4$ catalyst (Pd: 1.1 wt%, K: 0.78 wt%) over the course of time. In Fig. 10, the spectrum around 1800 cm^{-1}, which was not observed on the pre-reduced catalyst by H_2 (as shown later in Fig. 11), was observed over the pre-reduced catalyst by CO. The peak at 1800 cm^{-1} is attributable to cobalt carbonyl, which includes 2–4 molecules of CO per adsorption site of Co [34–36]. The peak intensity then increased over the course of time, which means the increase of the amount of adsorbed CO. Results

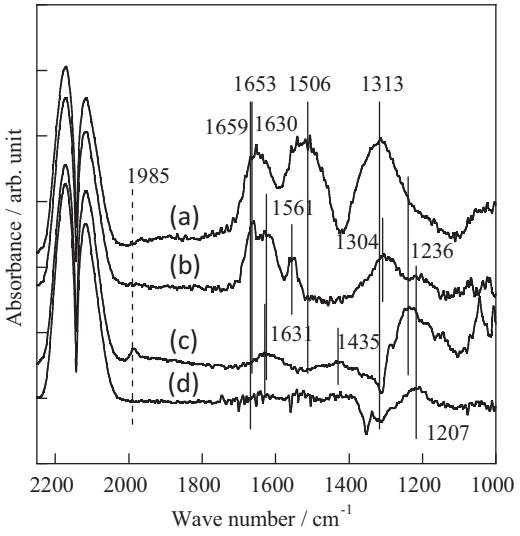

Fig. 11. DRIFT spectra of CO adsorbed at 298 K over $Pd/K/Co_3O_4$, Pd/Co_3O_4, K/Co_3O_4, and Co_3O_4: (a) $Pd/K/Co_3O_4$, (b) K/Co_3O_4, (c) Pd/Co_3O_4, and (d) Co_3O_4.

Table 3
Amount of initial products after flowing various gases containing $H_2{}^{18}O$.

	The amount of the initial products (mmol)								
Gas composition	H_2	H_2O	$H_2{}^{18}O$	CO	$C^{18}O$ ($\times10^4$)	Ar	CO_2	$C^{16}O^{18}O$($\times10^3$)	$C^{18}O_2$ ($\times10^5$)
$H_2{}^{18}O$	3.03	2.92	0.13	0.10	2.41	1.19	0.17	0.03	–
Reaction gas containing $H_2{}^{18}O$	4.01	1.58	0.11	0.09	2.68	0.59	0.19	1.66	6.95

suggest that CO adsorbed over metallic Co on the catalyst surface after pre-reduction, and that cobalt metal and CO produced the carbonyl intermediate. We presume that the initial high activity of pre-reduced catalyst by CO derived from the formation of cobalt carbonyl intermediate produced on the catalyst surface.

Fig. 11 shows DRIFT spectra for CO adsorption over various catalysts; $Pd/K/Co_3O_4$, Pd/Co_3O_4, K/Co_3O_4, Co_3O_4 (Pd: 1.1 wt%, K: 0.78 wt%). DRIFT measurements were conducted after reduction because the reaction gas was a reducing atmosphere. In Fig. 11, CO adsorption species around 2000–2200 cm^{-1} were gas-phase CO. The peak at 1985 cm^{-1} was observed for the spectra on Pd/Co_3O_4, which showed low catalytic activity, but the peak was not observed for that on $Pd/K/Co_3O_4$, which showed high catalytic activity. This peak at 1985 cm^{-1} is attributable to linear CO adsorption on Pd^0 [37,38]. Therefore, it is estimated that CO was adsorbed onto Pd metal over Pd/Co_3O_4, but no adsorption on Pd^0 as the linear form CO was observed over $Pd/K/Co_3O_4$. The linear form CO on Pd might have low activity because Pd/Co_3O_4 showed low catalytic activity. Over K/Co_3O_4, the peaks derived from carbonate species were observed at around 1300 and 1700 cm^{-1} [12,38–41]. The peak at around 1500 cm^{-1} was not observed over K/Co_3O_4, and the peak at 1561 cm^{-1} observed on K/Co_3O_4 was derived from ν(C=O) of bidentate carbonate [39]. Over Co_3O_4, a slight peak was observed at 1207 cm^{-1}, which derives from CO adsorbed on Co_3O_4 as carbonate species. The adsorbed site is most likely Co. The peak at 1236 cm^{-1} observed on Pd/Co_3O_4 is attributed to ν(OCO) of carbonate species. It is estimated that the adsorbed carbonate species on K/Co_3O_4 and Co_3O_4 has difficulty reacting with H_2O because K/Co_3O_4 and Co_3O_4 showed no WGS activity. The carbonate species observed at 1236 cm^{-1} over Pd/Co_3O_4, which showed low catalytic activity, also has low reactivity. Based on these results, the addition of potassium was inferred to promote the formation of carbonyl intermediate, and immediately converted to formate species.

DRIFT measurements were taken with H_2O or D_2O after CO flow over $Pd/K/Co_3O_4$ catalyst (Pd: 1.1 wt%, K: 0.78 wt%). Fig. 12 portrays results for the H–D exchange spectra. It was confirmed that the reaction proceeds via a Langmuir–Hinshelwood mechanism through formate, which contains H. The reaction for redox mechanism does not proceed through formate. In Fig. 12, compared to each spectrum after exposing H_2O, each spectrum of adsorption species after exposing D_2O was shifted to a lower wave number, from 1663 to 1650 cm^{-1}, from 1540 to 1519 cm^{-1}, and from 1337 to 1309 cm^{-1}. From these results, these spectra were attributable to adsorbed species including H. Then, the peak at 1663 cm^{-1} was attributed to the absorbed H_2O [38], the peak at 1540 cm^{-1} was attributed to ν_{as}(OCO) of bidentate formate, and the peak at 1337 cm^{-1} was attributed to ν_s(OCO) of bidentate formate [39,42].

Therefore, the reaction over $Pd/K/Co_3O_4$ catalyst proceeded through cobalt–carbonyl by CO adsorption, then it was converted to formate species immediately by the Langmuir–Hinshelwood mechanism.

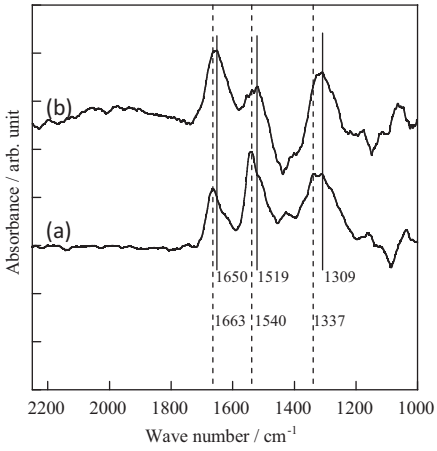

Fig. 12. DRIFT spectra of exposed in H_2O or D_2O after CO adsorption at 298 K over $Pd/K/Co_3O_4$: (a) exposed in H_2O and (b) exposed in D_2O.

4. Conclusion

We investigated the effects of Pd and K addition and the reaction mechanism over $Pd/K/Co_3O_4$ catalyst for the WGS reaction. It is important for a catalyst showing high catalytic activity that Pd and K exist nearby because $Pd/K/Co_3O_4$ catalysts prepared using impregnation showed higher initial catalytic activity than the catalysts prepared by physical mixture. TG measurements under the simulated reaction condition revealed that the structure of the support during the reaction was reduced to Co metal and that the reducibility of the support was promoted by the addition of Pd. EXAFS analyses showed the formation of Pd–Co alloy on $Pd/K/Co_3O_4$, and supported potassium donated electrons to Pd–Co alloy which enhanced the electron density of Pd and Co. The CO adsorption state over Pd and Co was changed by electron donation from K, and carbonyl and formate intermediate was observed on $Pd/K/Co_3O_4$ catalyst by in situ DRIFT. Pre-reduced $Pd/K/Co_3O_4$ catalyst by CO showed high catalytic activity for the WGS reaction by virtue of the formation of cobalt carbonyl and then formate intermediate. The intermediate plays an important role in the high catalytic activity on $Pd/K/Co_3O_4$ catalyst for the WGS reaction.

References

[1] C. Ratnasamy, J.P. Wagner, Catal. Rev. 51 (2009) 325–440.
[2] D. Mendes, A. Mendes, L.M. Madeira, A. Iulianelli, J.M. Sousa, A. Basile, Asia-Pac. J. Chem. Eng. 5 (2009) 111–137.
[3] J.R. Ladebeck, J.P. Wagner, Handbook Fuel Cells—Fundamentals, Technol. Appl. (2010) 1–12.
[4] D.S. Newsome, P. Kellogg, Catal. Rev. Sci. Eng. 21 (1980) 275–318.
[5] M.V. Twigg, M.S. Spencer, Appl. Catal. A: Gen. 212 (2001) 161–174.
[6] M. Haruta, S. Tsubota, T. Kobayashi, H. Kageyama, M.J. Genet, B. Delmon, J. Catal. 144 (1993) 175–192.
[7] D. Andreeva, V. Idakiev, T. Tabakova, A. Andreev, R. Giovanoli, Appl. Catal. A: Gen. 134 (1996) 275–283.
[8] A. Basinska, F. Domka, Appl. Catal. A: Gen. 179 (1999) 241–246.
[9] T. Bunluesin, R.J. Gorte, G.W. Graham, Appl. Catal. B: Environ. 15 (1998) 107–114.
[10] A. Luengnaruemitchai, S. Osuwan, E. Gulari, Catal. Commun. 4 (2003) 215–221.
[11] D. Andreeva, Gold Bull. 35 (2002) 82–88.
[12] J.M. Pigos, C.J. Brooks, G. Jacobs, H. Davis, Appl. Catal. A: Gen. 328 (2007) 14–26.
[13] H.N. Evin, G. Jacobs, J. Ruiz-Martinez, U.M. Graham, A. Dozier, G. Thomas, B.H. Davis, Catal. Lett. 122 (2008) 9–19.
[14] P. Panagiotopoulou, D.I. Kondarides, J. Catal. 267 (2009) 57–66.
[15] X. Zhu, T. Hoang, L.L. Lobban, R.G. Mallinson, Catal. Lett. 129 (2009) 135–141.
[16] Y. Zhai, D. Pierre, R. Si, A. Deng, P. Ferrin, A.U. Nilekar, G. Peng, J.A. Herron, D.C. Bell, H. Saltsburg, M. Mavrikakis, M. Flytzani-Stephanopopoulos, Science 329 (2010) 1633–1636.

[17] Y. Sekine, T. Chihara, R. Watanabe, Y. Sakamoto, M. Matsukata, E. Kikuchi, Catal. Lett. 140 (2010) 184–188.
[18] R. Watanabe, Y. Sakamoto, K. Yamamuro, S. Tamura, E. Kikuchi, Y. Sekine, Appl. Catal. A: Gen. 457 (2013) 1–11.
[19] K. Yamamuro, S. Tamura, R. Watanabe, Y. Sekine, Catal. Lett. 143 (2013) 339–344.
[20] F. Diehl, A.Y. Khodakov, Oil Gas Sci. Technol. 64 (2009) 11–24.
[21] A. Caballero, J.P. Espinós, A. Fernández, L. Soriano, A.R. González-Elipe, Surf. Sci. 364 (1996) 253–265.
[22] A. Miyakoshi, A. Ueno, M. Ichikawa, Appl. Catal. A: Gen. 219 (2001) 249–258.
[23] K. Asano, C. Ohnishi, S. Iwamoto, Y. Shioya, M. Inoue, Appl. Catal. B: Environ. 78 (2008) 242–249.
[24] M. Brun, A. Berthet, J.C. Bertolini, J. Electron. Spectrosc. Relat. Phenom. 104 (1999) 55–60.
[25] G. Pekiridis, K. Kaklidis, M. Konsolakis, E.F. Iliopoulou, I.V. Yentekakis, G.E. Marnellos, Top. Catal. 54 (2011) 1135–1142.
[26] A.F. Carlsson, M. Naschitzki, M. Bäumer, H.-J. Freund, J. Phys. Chem. B 107 (2003) 778–785.
[27] M. Krawczyk, J.W. Sobczak, Appl. Surf. Sci. 235 (2004) 49–52.
[28] L. Zhang, K. Lee, J. Zhang, Electrochim. Acta 52 (2007) 3088–3094.
[29] A.A. Khassin, T.M. Yurieva, V.V. Kaichev, V.I. Bukhtiyarov, A.A. Budneva, E.A. Paukshtis, V.N. Parmon, J. Mol. Catal. A: Chem. 175 (2001) 189–204.
[30] S.C. Petitto, E.M. Marsh, G.A. Carson, M.A. Langell, J. Mol. Catal. A: Chem. 281 (2008) 49–58.
[31] W. Ma, G. Jacobs, Y. Ji, T. Bhatelia, D.B. Bukur, S. Khalid, B.H. Davis, Top. Catal. 54 (2011) 757–767.
[32] B. Mierzwa, Z. Kaszkur, B. Moraweck, J. Pielaszek, J. Alloys Compd. 286 (1999) 93–97.
[33] H. Wang, W. Zhou, J-X. Liu, R. Si, G. Sun, M-Q. Zhong, H-Y. Su, H-B. Zhao, J.A. Rodriguez, S.J. Pennycook, J-C. Idrobo, W-X. Li, Y. Kou, D. Ma, J. Am. Chem. Soc. 135 (2013) 4149–4158.
[34] R.L. Schneider, R.F. Howe, K.L. Watters, Inorg. Chem. 23 (1984) 4593–4599.
[35] S. Suvanto, T.A. Pakkanen, J. Mol. Catal. A: Chem. 125 (1997) 91–96.
[36] F. Morales, E. Smit, F.M.F. Groot, T. Visser, B.M. Weckhuysen, J. Catal. 246 (2007) 91–99.
[37] H. Zhu, Z. Qin, W. Shan, W. Shen, J. Wang, J. Catal. 233 (2005) 41–50.
[38] G.G. Olympiou, C.M. Kalamaras, C.D. Zeinalipour-Yazdi, A.M. Efstathiou, Catal. Today 127 (2007) 304–318.
[39] T. Shido, Y. Iwasawa, J. Catal. 141 (1993) 71–81.
[40] D.I. Kondarides, T. Chafik, X.E. Verykios, J. Catal. 191 (2000) 147–164.
[41] R. Xu, H.C. Zeng, J. Phys. Chem. B 107 (2003) 12643–12649.
[42] G. Jacobs, L. Williams, U. Graham, G.A. Thomas, D.E. Sparks, B.H. Davis, Appl. Catal. A: Gen. 252 (2003) 107–118.